

## Supplementary Information for

# Monobody inhibitor selective to the phosphatase domain of SHP2 and its use as a probe for quantifying SHP2 allosteric regulation

Fern Sha<sup>1,5</sup>, Kohei Kurosawa<sup>1,2,5</sup>, Eliezra Glasser<sup>2,5</sup>, Gayatri Ketavarapu<sup>2,5</sup>, Samara Albazzaz<sup>1</sup>, Akiko Koide<sup>1,2,3</sup>, Shohei Koide<sup>1,2,4\*</sup>

<sup>1</sup>Department of Biochemistry and Molecular Biology, The University of Chicago, Chicago, IL 60637.

<sup>2</sup>Perlmutter Cancer Center, New York University Langone Health, New York, NY 10016.

<sup>3</sup>Department of Medicine, New York University Grossman School of Medicine, New York, NY 10016.

<sup>4</sup>Department of Biochemistry and Molecular Pharmacology, New York University Grossman School of Medicine, New York, NY 10016.

<sup>5</sup>Equal contribution.

\*Correspondence to: Shohei.Koide@nyulangone.org

Content

Supplementary Tables 1 and 2.

Supplementary Figures 1–6.

**Supplementary Table 1.** Kinetic parameters for BLI measurements.

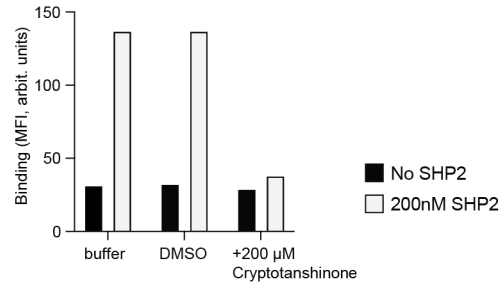
<b>Figure 1</b>						
<b>Mb11–analyte</b>	<b><math>K_D</math> (M)</b>	<b><math>K_D</math> Error</b>	<b><math>k_a</math> (1/Ms)</b>	<b><math>k_a</math> Error</b>	<b><math>k_d</math> (1/s)</b>	<b><math>k_d</math> Error</b>
SHP2 WT PTP	2.70E-09	9.70E-12	6.40E+05	1.60E+03	1.70E-03	4.60E-06
SHP2 C459S PTP	1.20E-07	1.60E-09	5.20E+05	6.50E+03	6.40E-02	3.40E-04
SHP1 PTP	1.00E-07	4.70E-10	5.40E+05	2.10E+03	5.40E-02	1.40E-04
PTP1B	9.00E-09	2.60E-09	1.90E+05	4.80E+04	1.70E-03	2.50E-04
<b>Mb13–analyte</b>						
SHP2 WT PTP	2.40E-09	9.40E-12	3.40E+05	5.50E+02	8.30E-04	3.00E-06
SHP2 C459S PTP	7.50E-10	6.60E-12	3.70E+05	4.90E+02	2.80E-04	2.40E-06
SHP1 PTP	2.80E-07	3.80E-09	4.40E+05	4.60E+03	1.20E-01	1.10E-03
PTP1B	7.70E-12	N/D	3.20E+04	5.40E+03	2.40E-07	N/D
<b>Figure 3 (Mb13–Analyte)</b>						
SHP2 WT	1.30E-07	4.50E-10	8.60E+03	1.90E+01	1.10E-03	2.90E-06
SHP2 $\Delta$ N-SH2	7.06E-09	2.19E-11	2.74E+05	5.54E+02	1.94E-03	4.55E-06
SHP2 WT N-tag	2.80E-08	5.70E-10	7.00E+03	2.50E+01	1.90E-04	3.90E-06
SHP2 E76K	5.70E-09	1.40E-11	2.50E+05	3.90E+02	1.40E-03	2.80E-06
SHP2 C459S	1.20E-09	7.80E-12	4.70E+05	6.60E+02	5.60E-04	2.60E-06
SHP2 C459E	2.08E-7	6.42E-10	1.71E+04	4.37E+01	3.56E-03	6.16E-06
SHP2 WT +pY	1.60E-09	1.60E-11	9.50E+04	5.30E+02	1.50E-04	1.30E-06
SHP2 E76K +pY	1.60E-09	8.80E-12	4.80E+05	1.70E+03	7.60E-04	3.30E-06
SHP2 C459S +pY	4.00E-10	1.70E-12	4.30E+05	3.70E+02	1.70E-04	7.00E-07
SHP2 C459E +pY	9.34E-10	5.22E-12	2.65E+05	1.03E+3	2.48E-04	1.00E-06
<b>Figure 4 (Mb13–Analyte)</b>						
SHP2 WT +SHP099	<1.0E-12	N/D	1.50E+08	3.40E+07	6.30E-07	N/D
SHP2 E76K +SHP099	2.00E-09	3.80E-11	3.00E+05	3.80E+03	6.00E-04	8.50E-06
SHP2 C459S +SHP099	6.90E-10	3.10E-11	2.90E+05	4.00E+03	2.00E-04	8.60E-06
SHP2 WT +CS3	9.30E-09	3.60E-10	7.80E+04	2.90E+03	7.30E-04	7.50E-06
SHP2 E76K +CS3	8.60E-10	3.50E-12	5.10E+05	8.90E+02	4.40E-04	1.60E-06
SHP2 C459S +CS3	6.80E-10	3.20E-12	3.50E+05	5.30E+02	2.40E-04	1.10E-06
SHP2 WT N-tag +CS3	4.70E-12	N/D	5.00E+04	3.40E+03	2.30E-07	N/D
SHP2 WT +NSa1	8.50E-09	8.00E-11	2.10E+05	1.90E+03	1.80E-03	5.10E-06
SHP2 E76K +NSa1	2.90E-09	1.90E-11	5.50E+05	2.90E+03	1.60E-03	5.70E-06
SHP2 C459S +NSa1	1.80E-09	1.20E-11	3.60E+05	1.50E+03	6.60E-04	3.10E-06
<b>Supple. Fig. 2 (Mb13–Analyte)</b>						
SHP2 PTP + 1mM citrate	6.69E-09	5.17E-11	2.00E+05	8.42E+02	1.33E-03	8.63E-06
Oxidized SHP2 PTP	2.50E-8	1.84E-10	4.45E+04	2.14E+02	1.11E-03	6.18E-06

Errors indicated are from fitting of a 1:1 binding model.

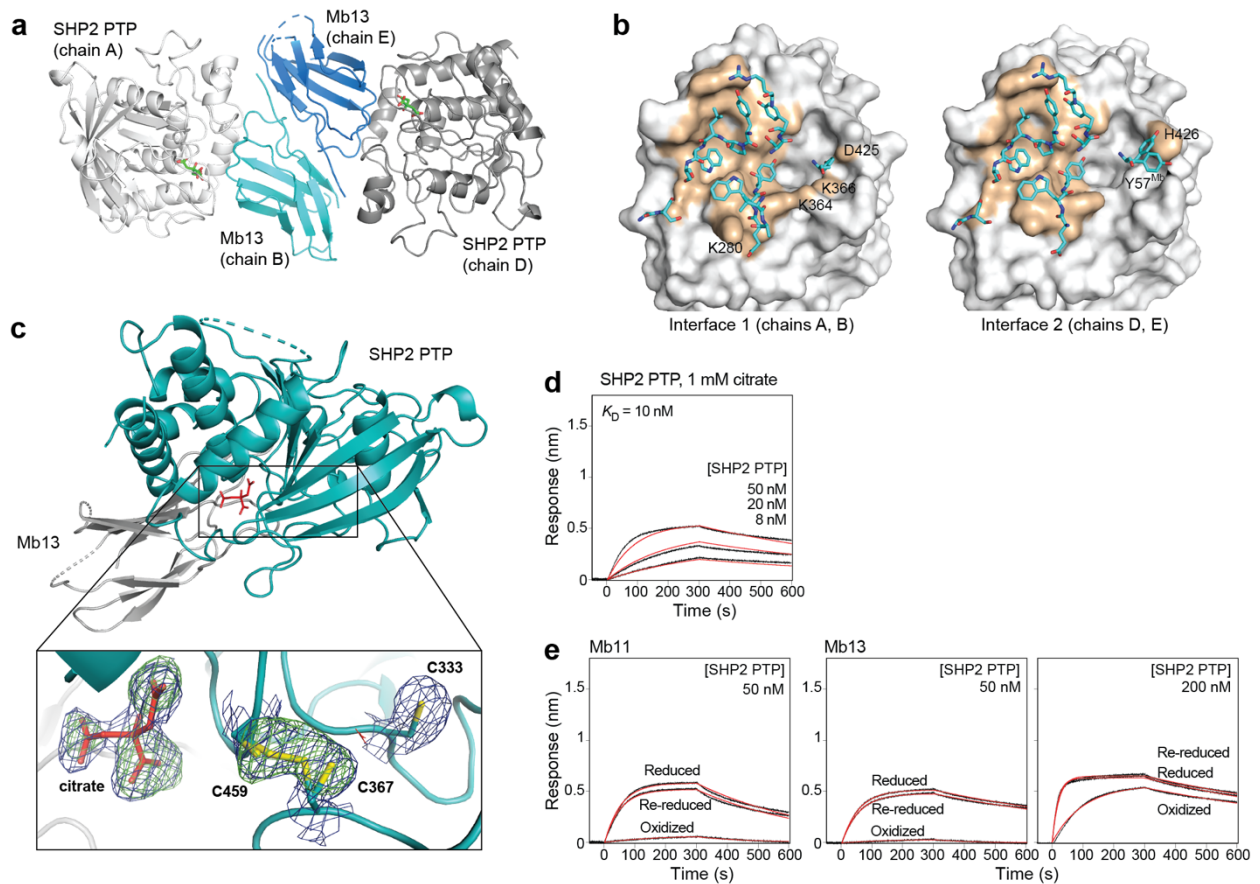
**Supplementary Table 2.** Buried surface areas for the two Mb13–PTP complexes (chains A and B, and chains D and E, respectively) in the asymmetric unit

PTP				Mb13			
	chain A	chain D	Difference (A-D)		chain B	chain E	difference (B-E)
PHE 251	6.9	8.7	-1.7	GLY 2	12.6	18.5	-5.9
GLU 252	35.8	40.5	-4.8	SER 3	10.3	13.1	-2.8
GLN 255	48.0	46.7	1.3	SER 5	2.1	0	2.1
GLN 256*	32.3	36.6	-4.3	<b>VAL 28</b>	<b>10.0</b>	<b>0</b>	<b>10.0</b>
GLU 258	24.4	22.9	1.5	<b>ASP 29</b>	<b>11.3</b>	<b>0.6</b>	<b>10.7</b>
CYS 259*	43.5	46.4	-2.8	<b>GLU 30</b>	<b>84.4</b>	<b>61.8</b>	<b>22.6</b>
LYS 260	2.0	3.7	-1.7	TRP 31	48.9	42.8	6.1
LEU 261*	23.4	20.4	3.0	TYR 32	112.9	112.1	0.8
ARG 265	23.5	27.7	-4.2	SER 34	29.7	32.2	-2.5
GLN 269	25.5	33.4	-8.0	TYR 35	58.2	58.3	-0.1
LYS 274	3.7	0.0	3.7	ARG 37	22.9	27.7	-4.8
ASN 277	7.9	2.8	5.1	GLU 51	0.0	2.0	-2.0
ARG 278	15.5	10.2	5.3	PRO 55	4.2	0.2	4.0
TYR 279	48.9	46.5	2.4	<b>TYR 57</b>	<b>63.4</b>	<b>15.9 (42.4)</b>	<b>47.5 (21.0)</b>
<b>LYS 280</b>	<b>88.8</b>	<b>36.3</b>	<b>52.5</b>	TYR 77	0.6	1.2	-0.6
ASN 281	100.6	103.3	-2.6	TYR 79	41.7	37.3	4.4
ILE 282	23.1	25.1	-2.0	PRO 80	26.2	25.9	0.3
<b>LYS 364</b>	<b>17.2</b>	<b>0.0</b>	<b>17.2</b>	LEU 81	72.9	71.4	1.5
<b>LYS 366</b>	<b>15.6</b>	<b>0.0</b>	<b>15.6</b>	TRP 82	180.1	181.9	-1.8
<b>ASP 425</b>	<b>18.7</b>	<b>0.0</b>	<b>18.7</b>	SER 83	22.0	27.5	-5.5
<b>HIS 426</b>	<b>9.5</b>	<b>18.3 (42.8)</b>	<b>-8.8 (-33.3)</b>				
SER 460	0.5	0.4	0.1				
ALA 461	11.9	12.1	-0.2				
ILE 463	10.4	9.7	0.7				
GLY 464	3.4	3.2	0.3				
ARG 465	3.7	0.0	3.7				
SER 502	8.6	8.2	0.5				
GLY 503	6.1	5.5	0.7				
GLN 506	61.8	61.1	0.7				
THR 507	28.3	28.0	0.3				
GLU 508	3.1	2.7	0.4				

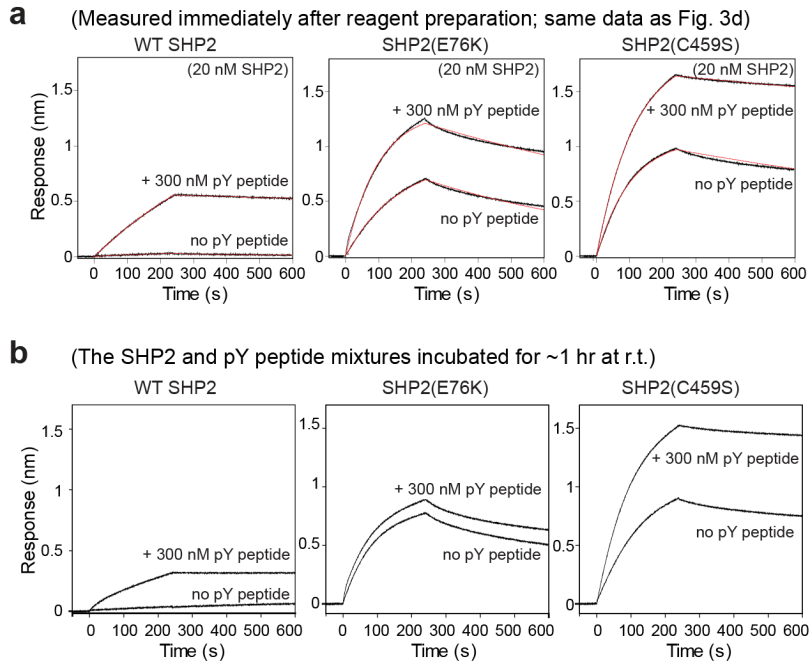
Buried surface areas in Å<sup>2</sup> were calculated using the PEBEPIISA server. Values for the two rotamers, A and B, of Tyr57 of Mb13 are shown, with the values for B in the parentheses. Residues that show a difference of ≥10 Å<sup>2</sup> are indicated in bold. Residues that are different between SHP2 and SHP1 are marked with an asterisk.



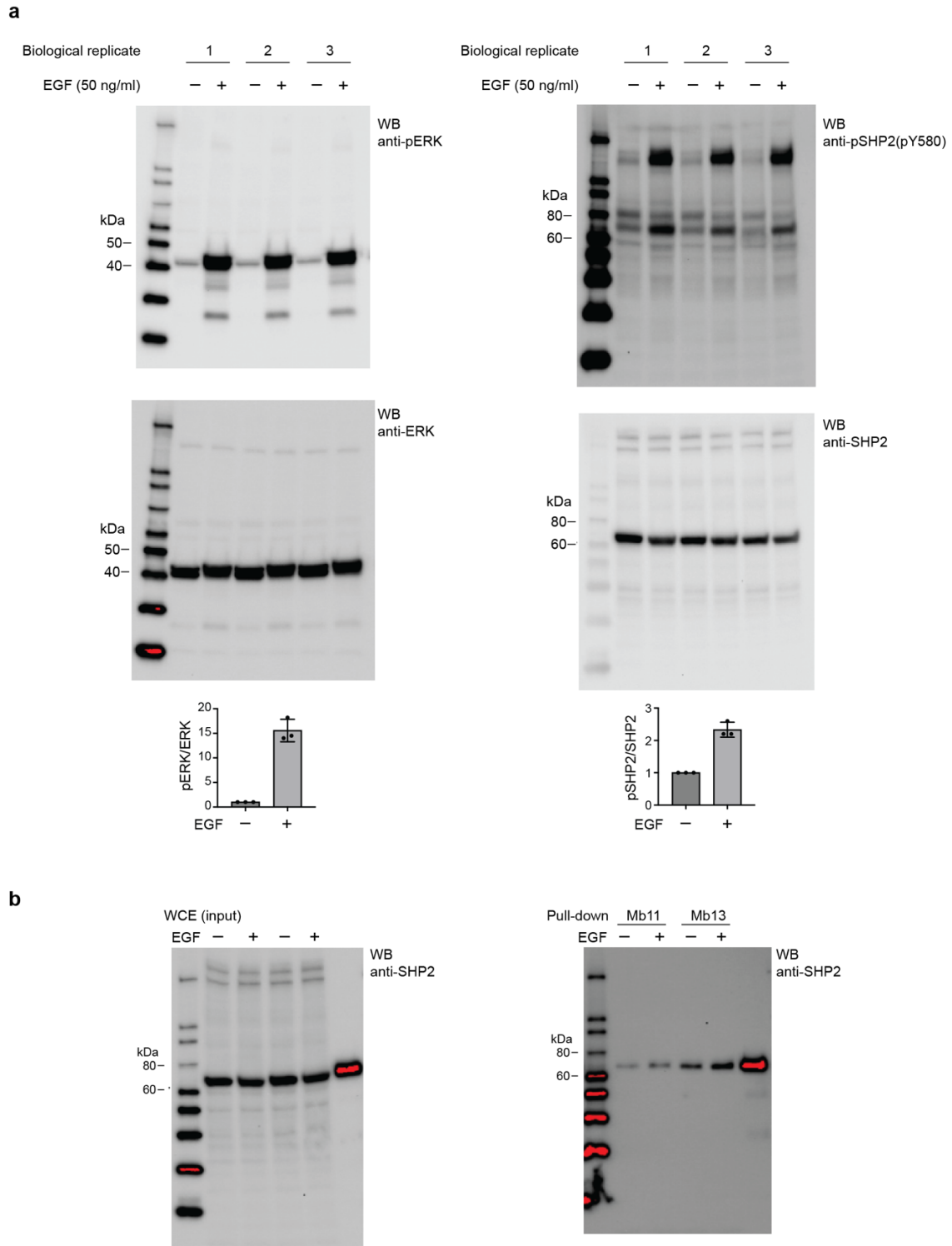
**Supplementary Figure 1.** Competition experiment showing that cryptotanshinone is a competitive inhibitor of Mb13 for binding to SHP2 PTP. Binding signals of SHP2 to Mb13 in the absence or presence of 100  $\mu$ M cryptotanshinone are shown.



**Supplementary Figure 2.** Crystal structure of the SHP2 PTP–Mb13 complex. **(a)** The asymmetric unit containing two copies of the PTP–Mb13 complex shown as cartoon models. **(b)** A comparison of the PTP–Mb13 interface between the two complexes in the asymmetric unit. PTP is represented as a surface model with the epitope in brown and residues within the paratope of Mb13, as defined as those within 5 Å of PTP atoms, are represented as sticks. PTP residues that exhibit substantial differences between the two complexes in the asymmetric unit (Supplementary Table 2) are labeled. Y57 of Mb13 that shows two rotamers is also labeled. **(c)** Electron density in the active site of SHP2 PTP. The  $2F_o-F_c$  map is shown in blue mesh (contoured at  $1.0\sigma$  and carved at  $1.7\text{Å}$ ) for the citrate ion and the side chains of C333, C367, and C459. The side chains of C367 and C459 were modeled with partial occupancies as a mixture of reduced and disulfide forms. The  $F_o-F_c$  omit map is shown in green mesh (contoured at  $3.0\sigma$  and carved at  $1.9\text{Å}$ ) after refinement with the citrate ion and  $\gamma$ S atoms of C367 and C459 omitted. **(d)** BLI sensorgrams of SHP2 PTP binding to Mb13 on the sensor tip in the presence of 1 mM citrate. The  $K_D$  value was derived from global fitting of a 1:1 binding model. The red curves show the best fit. **(e)** Sensorgrams of the SHP2 PTP domain binding to Mb11 or Mb13 before (“Reduced”) and after (“Oxidized”) treatment with  $\text{H}_2\text{O}_2$ , and after subsequent treatment with DTT (“Re-reduced”). For Mb13, experiments using 50 nM and 200 nM SHP2 PTP samples are shown.

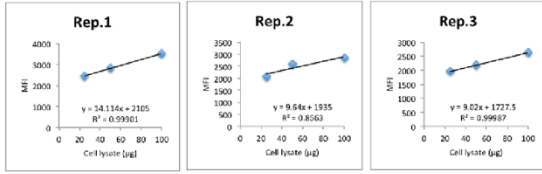


**Supplementary Figure 3.** Dephosphorylation of a tandem pY peptide by SHP2(WT) and SHP2(E76K) but not by SHP2(C459S). **(a)** BLI sensorgrams of SHP2 proteins binding to Mb13, as shown in Fig. 3d. **(b)** The same experiments after the pY peptide was incubated with the SHP2 proteins for ~1 hr, in the absence of Mb13. The activation activity of the pY peptide was reduced after incubation with active SHP2, but not with the PTP-dead mutant, C459S.

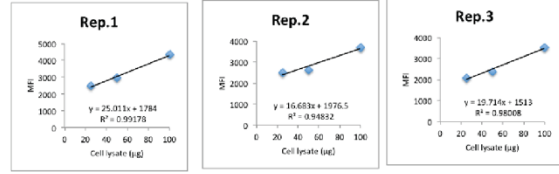


**Supplementary Figure 4. (a)** Activation of the MAP kinase signaling pathway and SHP2 phosphorylation upon EGF treatment of HEK293 cells. **(b)** Full-length gel images for Fig. 5a.

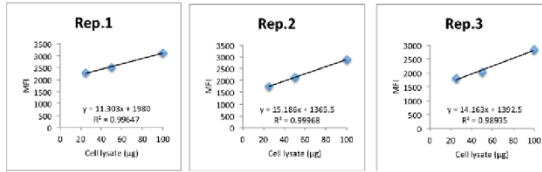
MB11-unstimulated



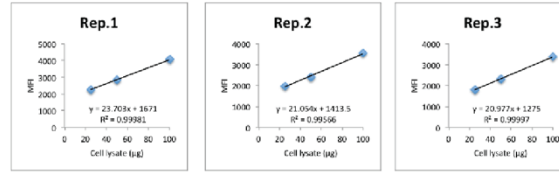
MB11-EGF



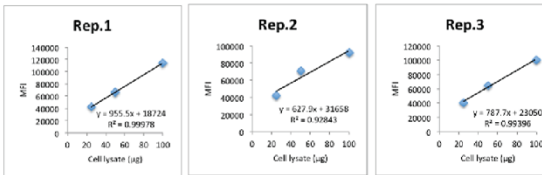
MB13-unstimulated



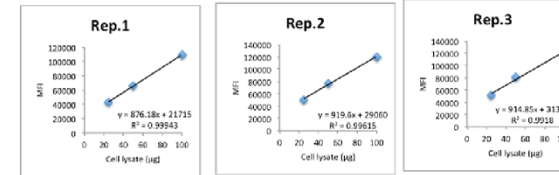
MB13-EGF



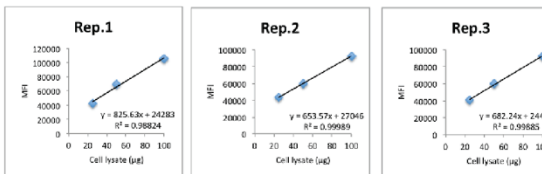
MB11-unstimulated



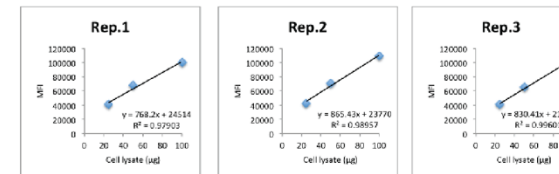
MB11-EGF



MB13-unstimulated

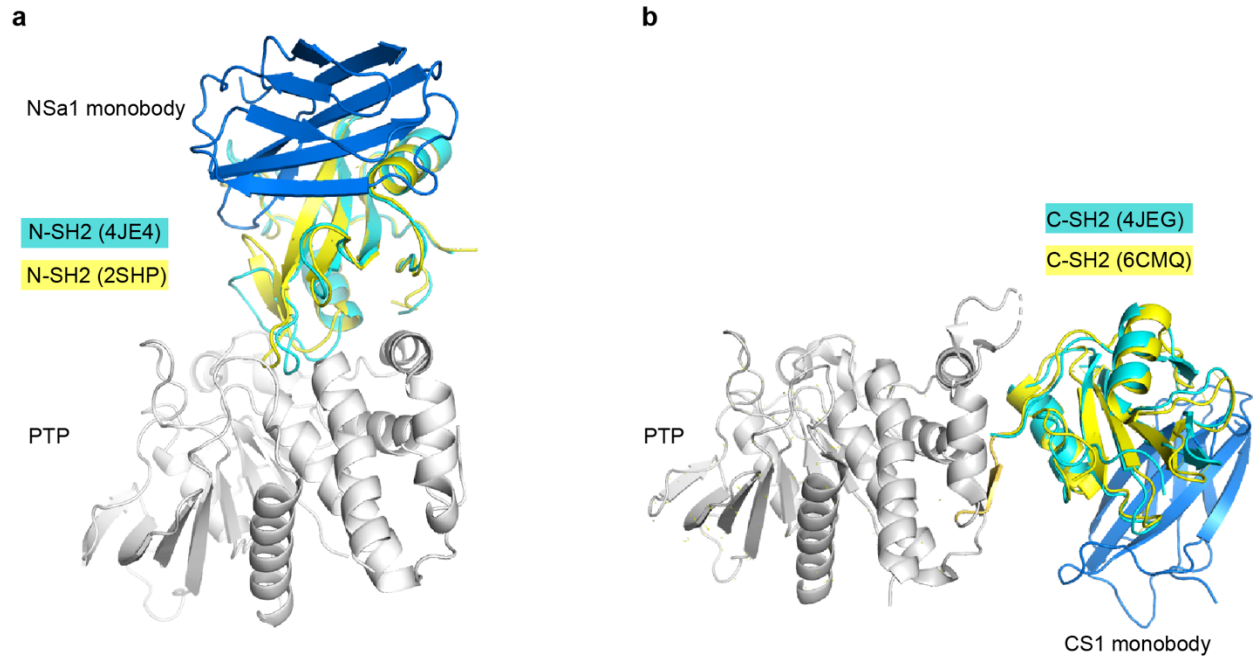


MB13-EGF



**Supplementary Figure 5.** Raw data for Fig. 5b. Flow cytometry signal intensities for the monobody captured SHP2 and the determination of their slopes with respect to the amount of lysate input.





**Supplementary Figure 6.** Potential mechanisms for the monobodies directed to the SH2 domains to preferentially stabilize the open conformation of SHP2. **(a)** Superposition of the N-SH2 domain in the closed conformation of full-length SHP2 (PDB ID: 2SHP) with the N-SH2 domain in the N-SH2-NSa1 monobody complex (PDB ID: 4JE4). The C-SH2 domain was omitted for clarity. **(b)** Superposition of the C-SH2 domain in the  $\Delta$ N-SH2 SHP2 fragment (PDB ID: 6CMQ, chain A) with the C-SH2 domain in the C-SH2-CS1 monobody complex (PDB ID: 4JEG). The CS1 monobody does not create steric clashes with the PTP domain.